jove

Identifying Bone Marrow Microenvironmental Populations in Myelodysplastic Syndrome and Acute Myeloid Leukemia

Christina M. Kaszuba[1,2], **Benjamin J. Rodems**[1,3], **Sonali Sharma**[1,3], **Edgardo I. Franco**[1,2], **John M. Ashton**[1,3,4], **Laura M. Calvi**[1,5], **Jeevisha Bajaj**[1,3]

[1] Wilmot Cancer Institute, University of Rochester Medical Center [2] Department of Biomedical Engineering, University of Rochester [3] Department of Biomedical Genetics, University of Rochester Medical Center [4] Genomics Research Center, University of Rochester Medical Center [5] Division of Endocrinology and Metabolism, Department of Medicine, University of Rochester Medical Center

Corresponding Author

Jeevisha Bajaj
Jeevisha_Bajaj@urmc.rochester.edu

Citation

Kaszuba, C.M., Rodems, B.J., Sharma, S., Franco, E.I., Ashton, J.M., Calvi, L.M., Bajaj, J. Identifying Bone Marrow Microenvironmental Populations in Myelodysplastic Syndrome and Acute Myeloid Leukemia. *J. Vis. Exp.* (201), e66093, doi:10.3791/66093 (2023).

Date Published

November 10, 2023

DOI

10.3791/66093

URL

jove.com/video/66093

Abstract

The bone marrow microenvironment consists of distinct cell populations, such as mesenchymal stromal cells, endothelial cells, osteolineage cells, and fibroblasts, which provide support for hematopoietic stem cells (HSCs). In addition to supporting normal HSCs, the bone marrow microenvironment also plays a role in the development of hematopoietic stem cell disorders, such as myelodysplastic syndromes (MDS) and acute myeloid leukemia (AML). MDS-associated mutations in HSCs lead to a block in differentiation and progressive bone marrow failure, especially in the elderly. MDS can often progress to therapy-resistant AML, a disease characterized by a rapid accumulation of immature myeloid blasts. The bone marrow microenvironment is known to be altered in patients with these myeloid neoplasms. Here, a comprehensive protocol to isolate and phenotypically characterize bone marrow microenvironmental cells from murine models of myelodysplastic syndrome and acute myeloid leukemia is described. Isolating and characterizing changes in the bone marrow niche populations can help determine their role in disease initiation and progression and may lead to the development of novel therapeutics targeting cancer-promoting alterations in the bone marrow stromal populations.

Introduction

The bone marrow microenvironment consists of hematopoietic cells, non-hematopoietic stromal cells, and the extracellular matrix[1,2]. This microenvironment can promote hematopoietic stem cell self-renewal, regulate lineage differentiation, and provide structural and mechanical support to the bone tissue[1,2,3,4,5]. The stromal niche includes osteolineage cells, fibroblasts, nerve cells, and endothelial cells[6], while the hematopoietic niche consists of the lymphoid and myeloid populations[1,2,3]. In addition to supporting normal HSCs, the bone marrow microenvironment

can also play a role in the development of hematopoietic stem cell disorders such as MDS and AML[7,8,9,10,11]. Mutations in osteolineage cells have been shown to promote the development of MDS, AML, and other myeloproliferative neoplasms[10,12,13,14].

Myelodysplastic syndromes are a group of pre-leukemic disorders that arise from mutations in hematopoietic stem cells. MDS is frequently associated with a block in HSC differentiation and the production of dysplastic cells, which can often lead to bone marrow failure. MDS is the most commonly diagnosed myeloid neoplasm in the United States and is associated with a 3-year survival rate of 35%-45%[15]. MDS is often associated with a high risk of transformation to acute myeloid leukemia. This can be a fatal complication, as MDS-derived AML is resistant to most therapies and likely to relapse. AML that arises *de novo* due to translocations or mutations in hematopoietic stem and progenitors is also often resistant to standard chemotherapy[16,17]. Since MDS and AML are primarily diseases of the elderly, with the majority diagnosed over the age of 60 years, most patients are ineligible for curative bone marrow transplants. There is, thus, a significant need to identify novel regulators of disease progression. Since the bone marrow microenvironment can provide support for malignant cells[14], defining changes in the bone marrow niche with disease progression may lead to the identification of novel therapeutics aimed at inhibiting tumor niche remodeling. There is, therefore, a significant need to identify novel regulators of disease progression. To this end, it is critical to identify and characterize changes in the bone marrow stromal cell populations that may provide support for the malignant cells.

Several murine models of AML and MDS have been generated and can be used to study changes in the bone marrow microenvironment during disease initiation and progression[6,1,19,20,21,22]. Here, protocols to identify changes in the bone marrow stromal cell populations using murine models of retrovirally induced AML[6,20], as well as the commercially available Nup98-HoxD13 (NHD13) model of high-risk MDS to AML transformation[19], are described. Mice transplanted with *de novo* AML cells succumb to the disease in 20-30 days[6]. The NHD13 mice develop cytopenias and bone marrow dysplasia around 15-20 weeks, which eventually transforms into AML, and nearly 75% of the mice succumb to the disease around 32 weeks. To analyze the murine model bone marrow microenvironment populations, bones are harvested, bone marrow and bone spicules are digested using enzymatic digestion, and the cells are then enriched for CD45-/Ter119- non-hematopoietic populations by magnetic sorting. While similar analyses have been previously described[11,13,22,23,24,25], they often focus on either the bone marrow or the bone and do not incorporate cells from both sources in their analyses. The combined characterization of these populations, in conjunction with gene expression analyses, can provide a comprehensive understanding of how the cellular hematopoietic microenvironment provides support for disease initiation and progression (**Figure 1**). While the protocol described below focuses on retrovirally induced AML model and a genetic MDS model, these strategies can be easily adapted to study changes in the bone marrow niche of any murine model of interest.

Protocol

All animal experiments were conducted in accordance with protocols approved by the University of Rochester University Committee on Animal Resources. Mice were bred and maintained in the animal care facilities at the University

of Rochester. To model high-risk MDS, the commercially available NHD13 murine model[19] is employed. In this model, bone marrow stromal cells are analyzed in female NHD13 mice at 8 weeks of age, before disease onset. *De novo* AML is generated as previously described[6,11,20]. The oncogenes used to induce AML, such as MLL-AF9 and NRas, are tagged with GFP or YFP, allowing for the analysis of the non-leukemic GFP- bone marrow populations using flow cytometry. In brief, 10-week-old female C57BL/6J mice are transplanted with murine GFP/YFP+ AML cells, and the bone marrow is harvested 2 weeks post-transplant. While female mice are used in this study for demonstration purposes, this protocol can be conducted with either male or female mice. It can also be carried out using either one femur or all long bones.

1. Bone marrow harvesting

NOTE: For details on the animal dissection protocol, please refer to Amend et al.[26].

1. Clean the mortar and pestle with 70% ethanol, rinse them with chilled FACS buffer (**Table 1**), and place them on ice to cool before starting the harvest. Also, place MACs buffer (**Table 1**) on the bench to allow it to reach room temperature.
2. Euthanize the animal following the institutional animal care and use guidelines and protocols.
3. On the benchtop, thoroughly spray the mouse with 70% ethanol until its fur is wet. Using forceps and curved scissors, lift the skin on the abdomen and make two incisions approximately 0.5 mm in length on both sides of the mouse, lateral from the abdomen. Next, make a 0.5 mm incision distal from the abdomen. Pull down to remove the skin and fur from the mouse's legs.
4. Place scissors perpendicular to the pelvis, press down while pulling up on the femur with forceps. The femoral head should detach from the pelvis. Separate the femur and tibia at the patellofemoral joint. Place the bones in FACS buffer in a 6-well plate on ice.
5. Remove tissue from the bones using laboratory-grade tissue and place the cleaned bones into a new 6-well plate with fresh FACS buffer on ice.
6. Place all bones into the mortar with 2-5 mL of FACS buffer so that all bones are immersed in the buffer (adjust the volume of buffer based on how many bones you are processing). Crush and grind the bones using the pestle in a circular motion until the bone marrow tissue is released.
7. Using a 3 mL syringe, homogenize the bone marrow by pulling up and flushing down the liquid from the mortar.
8. Using a 3 mL syringe, pull up the liquid from the mortar and filter it through a 70 µm cell strainer into a 50 mL tube on ice. Rinse the bone/tissue chunks from the filter back into the mortar with FACS buffer and return to step 1.7 to homogenize and strain a second time. This constitutes the bone marrow fraction.
9. Rinse the remaining bone pieces (spicules) back into the mortar with FACS buffer and flush them into a 15 mL tube using FACS buffer to ensure maximum cell yield. This is the bone spicules fraction.

2. Digestion of bone marrow

1. Centrifuge the bone marrow at 300 x *g* for 5 min at 4 °C. Decant and discard the supernatant.
2. Resuspend the bone marrow in 2 mL of the bone marrow digestion mixture (**Table 1**) and transfer it to a 15 mL tube. Incubate at 37 °C for 45 min on a rotator.

3. Add 10 mL of FACS buffer to stop the enzymatic digestion. Filter the mixture through a 70 µm cell strainer into a new 50 mL tube.
4. Pellet the mixture at 400 x *g* for 7 min at 4 °C.
5. Resuspend the bone marrow pellet in 1 mL of RBC lysis buffer (see **Table of Materials**). Incubate for 4 min on ice.
6. Add 10 mL of FACS buffer to stop the lysis. Filter the mixture through a 70 µm cell strainer into a new 50 mL tube.
7. Pellet the mixture at 300 x *g* for 5 min at 4 °C. Remove the supernatant and resuspend the pellet in 100 µL of FACS buffer.

3. Digestion of bone spicules

1. Vortex the bone spicules from step 1.9 and allow them to settle. Decant the supernatant and retain the bone at the bottom.
2. Resuspend the bone spicules in 1 mL of the bone spicule digestion mixture (**Table 1**).
3. Place the tubes on a tube rotator for 60 min at 37 °C.
4. Add 10 mL of FACS buffer to stop the enzymatic digestion. Filter the mixture through a 70 µm cell strainer into the 50 mL tube containing RBC-lysed and digested bone marrow.

4. Staining

1. Gently mix the bone spicules and bone marrow cell suspension.
2. Use 10 µL of the cell suspension to count the live cell number on a hemocytometer using 0.4% Trypan blue-based staining, as described in published protocols[27]. Collect 50,000 cells for an unstained control from the cell suspension.
3. Centrifuge the remaining cells at 300 x *g* for 5 min at 4 °C. Remove the supernatant and resuspend them in 100 µL of FACS buffer.
   NOTE: Antibodies can be titrated to determine the ideal dilution. Antibody selection (epitopes and fluorochromes) can be customized.
4. For staining with antibodies for magnetic depletion, add FC Block (1 µL per 25 x 10^6 cells), CD45-APC (10 µL per 25 x 10^6 cells), and Ter119-APC (4 µL per 25 x 10^6 cells) (see **Table of Materials**).
5. Incubate on ice for 20 min. Wash with FACS buffer, remove 50,000 cells (~50 µL) for the APC-stained control, centrifuge at 300 x *g* for 5 min at 4 °C, and resuspend in 100 µL of FACS buffer.
6. For staining of the cell suspension with microbeads for magnetic depletion, add mIgG (8 µL per 25 x 10^6 cells) and Anti-APC microbeads (20 µL per 25 x 10^6 cells) (see **Table of Materials**).
7. Incubate on ice for 20 min. Wash with 10 mL FACS buffer, centrifuge at 300 x *g* for 5 min at 4 °C.

5. Depletion of sample by magnetic sorting

NOTE: This step is carried out using a commercially available manual magnetic separator according to the manufacturer's instructions. This step can also be performed with an automated separator (see **Table of Materials**).

1. Prepare the LD column by washing it with 2 mL of MACs buffer (**Table 1**). Discard the effluent and change the collection tube.

2. Resuspend up to 1 x 10^8 cells in MACs buffer and filter them through a 5 mL test tube with a 35 µm cell strainer cap.
3. Place the LD column on the magnetic separator stand. Position a 5 mL test tube below the column to collect the eluate.
4. Add the cell suspension to the prepared LD column. Allow the negative fraction to flow through into the collection tube. Wash the column twice with 1 mL of MACs buffer, collecting the eluate in the same tube. This is the negative fraction used in step 5.6 below.
5. Remove the LD column from the magnetic separator stand and place it on a new 5 mL test tube. Use a pipette to dispense 3 mL of buffer into the column to flush out cells that have been positively labeled, using the column plunger.
6. Centrifuge the negative and positive fractions at 300 x *g* for 5 min at 4 °C. Resuspend them in 100 µL of FACS buffer.
7. Count 10 µL of the negative and positive fractions with 0.4% Trypan blue. The volumes for the osteo-analysis/ endothelial panel staining below will be based on this cell count.
8. Use 50,000 live cells from the positive fraction for flow cytometry gating controls.

6. Osteo-analysis/endothelial panel stain

NOTE: Compensation should be performed following standard flow cytometry protocols, including all appropriate staining and gating controls.

1. For staining of the CD45/Ter119 negative fraction (1 µL of each antibody per 1 x 10^6 cells), add CD31-PE-Cy7, Sca-1-BV421, CD51-PE, and CD140a-PE-Cy5 (see **Table of Materials**).
2. Incubate on ice for 20 min. Wash with 2 mL of FACS buffer, then centrifuge at 300 x *g* for 5 min at 4 °C.
3. Add 1 mL of FACS buffer and a 1:1000 dilution of PI for live/dead staining, then filter the sample through a 5 mL test tube with a 35 µm cell strainer cap.
4. Analyze the cells on a multi-color flow cytometer.

Representative Results

This article describes a flow cytometry-based method for analyzing bone marrow microenvironmental populations, such as the endothelial and mesenchymal stromal cells, from MDS and leukemia murine models (**Figure 1**). **Figure 2** depicts the gating strategy for detection of populations of interest, beginning with the selection of cells (P1) in the digested and CD45/Ter119 depleted fraction through forward and side scatter profile. Example gating of cells in a leukemia sample are shown in P1 (**Figure 2A**). Singlets are selected and doublets are excluded from this analysis, P2 (**Figure 2B**). **Figure 2C** shows gates to select propidium iodine negative live cells, P3. To focus on non-hematopoietic stromal populations, cells that are CD45-/Ter119-, P4 (APC, Y-axis) *vs*. SSC-A are selected (**Figure 2D**). This initial gating strategy is common for all samples to be analyzed.

The leukemia murine model is used to illustrate gating for endothelial cells in **Figures 2E-G**. **Figure 2E** depicts CD31 positive (Pe-Cy7, Y-axis) *vs*. SSC-A cells in a non-cancer control mouse as well as a leukemic mouse, gated through P4. Cells positively labeled with CD31 are endothelial cells, P5. In **Figure 2F**, gated through P5, arteriolar endothelial cells are identified as CD45-Ter119-CD31+Sca1+, P6, and

sinusoidal endothelial cells are identified as CD45-Ter119-CD31+Sca1-, P7 (BV421, Y-axis) *vs*. SSC-A.

Although this analysis focusses on non-leukemic bone marrow microenvironmental cells, it is also helpful to determine tumor burden. This can be done with a small fraction of undigested/non-depleted sample prior to initiating the experiment. In this experimental control (dashed lines) **Figure 2G**, P8 represents tumor burden in the sample and P9 represents the non-cancerous cells.

The MDS murine model is used to illustrate analysis of mesenchymal stromal cells in **Figure 2H-J**. **Figure 2H** depicts CD31 negative (Pe-Cy7, Y-axis) *vs*. SSC-A cells, gated through P4. Mesenchymal stromal cell populations in a wild-type control mouse and MDS mouse are shown in **Figure 2I**. Gated through P10, mesenchymal stromal cells are identified as CD45-Ter119-CD31-CD51+CD140a+, P11[3] (Pe, Y-axis; Pe-Cy5, X-axis). The experimental control (dashed lines), **Figure 2J** shows examples of single-color gating controls, CD51 single stain and CD140a single stain used to gate for the MSCs shown in the experimental samples in **Figure 2I**.

This data indicates that arteriolar endothelial cells significantly expand in the AML microenvironment, with a concomitant loss in the sinusoidal endothelial populations (**Figure 2F**), consistent with earlier studies using patient derived xenografts in immunodeficient mice[28]. It is likely that the small expansion in the mesenchymal stromal cells seen in the NHD13 mice at 8 weeks of age (**Figure 2I**) may increase at 16-20 weeks, when these mice start to display characteristics of MDS[25]. Although only the leukemia model is used to illustrate the endothelial cell population and the MDS murine model is used to illustrate the mesenchymal stromal cell populations, similar staining and gating strategies can be used to analyze the different microenvironmental populations in either of these models, or indeed, in any genetically engineered murine model of interest.

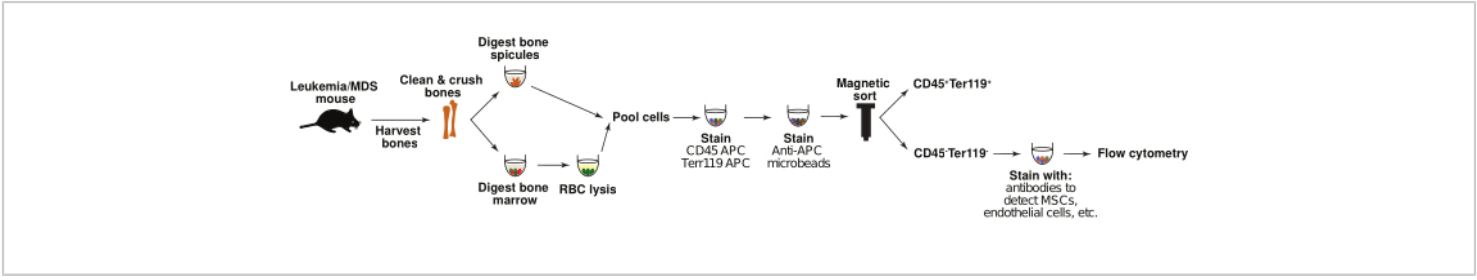

Figure 1: Isolation of bone marrow stromal cells. Schematic shows the process of isolating non-hematopoietic bone marrow stromal cells from control and leukemic mice. Briefly, bone spicules and bone marrow are digested separately and then pooled. The CD45-Ter119- population is enriched by magnetic sorting, and stained with antibody panels against populations of interest, such as mesenchymal stromal cells and endothelial cells. The cells are then analyzed by flow cytometry. Please click here to view a larger version of this figure.

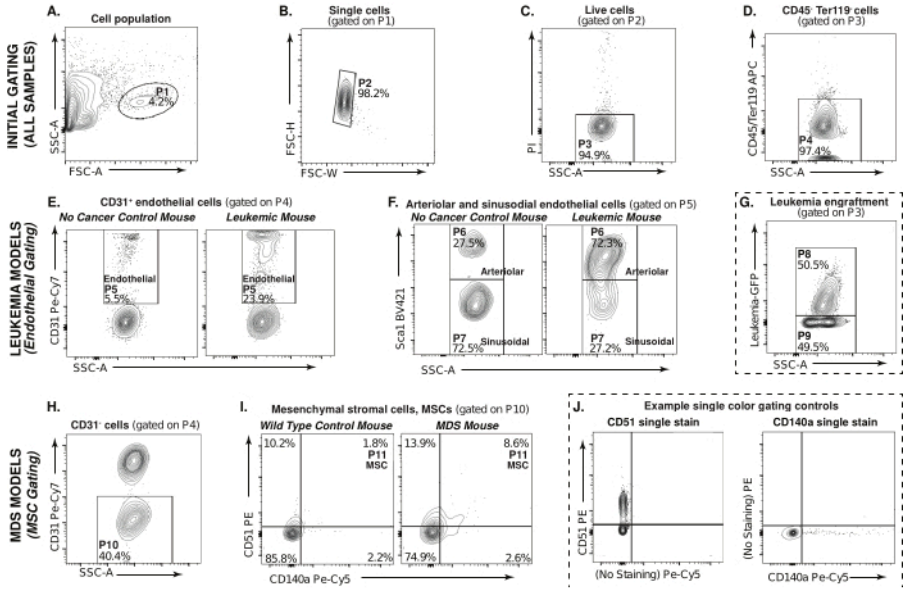

Figure 2: Gating strategy for non-hematopoietic bone marrow and stromal cells. (**A-D**) Flow cytometry gating strategy used to select digested, CD45-/Ter119-, non-hematopoietic populations (P4) in both the leukemia and MDS murine model. (**E**) Leukemia bone marrow endothelial cells (P5, CD31+) can be sub-divided as (**F**) Sca1+ arteriolar (P6) or Sca1- sinusoidal endothelial cells (P7). (**G**) Leukemia engraftment in an AML sample where P8 represents engraftment while P9 represents non-cancer cells. Dotted lines indicate that this plot is an experimental control. (**H**) Gated through P4, MDS bone marrow CD31- cells, P10 (**I**) Mesenchymal stromal cells (CD51+/CD140a+, P11). (**J**) Example single color gating controls, CD51 (left) and CD140a (right) used to determine the gates for mesenchymal stromal cells in (**I**). Please click here to view a larger version of this figure.

Solution	Reagent	Concentration	Amount to add
FACS buffer	HBSS	10x	100 mL
	EDTA	0.5 M	4 mL
	Fetal Bovine Serum	-	50 mL
	Water	-	848 mL
Bone marrow digestion mixture	HBSS	1x	2 mL
	DNase 1	1 µg/mL in 1x DPBS	20 µL
	Dispase II Powder	-	4 mg
	Collagenase Type IV	-	2 mg
Bone spicule digestion mixture	DPBS	1x	320 mL
	Collagenase Type 1	-	1 g
	Fetal Bovine Serum	-	80 mL
MACs buffer	BSA	66 g/mol	5 g
	DPBS	10x	100 mL
	EDTA	0.5 M	4 mL
	Water	-	896 L

Table 1: Composition of solutions and buffers used in the present study.

Discussion

Murine leukemia models have been extensively used to identify cell intrinsic and niche-driven signals that promote aggressive myeloid leukemia progression[6,19,21]. Here, a comprehensive flow cytometry-based protocol to define the cellular composition of the bone marrow microenvironment in murine models of MDS and AML is presented.

Prior to acquiring flow cytometric data from experimental samples, it is important to carefully compensate for fluorescence overlap. It is also essential to include all appropriate staining and gating controls. These steps will allow the experimenter to confirm that positive or negative antibody staining represents accurate expression of cell markers of interest and is not an artefact of fluorescence spectral overlap or autofluorescence. Although this protocol describes selected cell surface markers, the antibody panels can be expanded based on experimental need. For example, CD144 (Ve-Cadherin) can be administered *in vivo* before harvesting the mice and can serve as an additional specific marker of endothelial cells[5,29]. While the fluorophores and antibody clones indicated here can be changed, titrations should be carried out to determine their ideal dilution. To categorically define all cell populations in the bone marrow

niche, single cell RNA-sequencing can be used to establish the bone marrow niche landscape during MDS/AML initiation and progression[23,24,30].

It is critical to prepare the sample carefully as per the steps described in this protocol. When homogenizing the bones, it is crucial that the mortar and pestle are chilled, and all steps are carried out on ice to prevent cell death and to ensure high cell recovery. It is very important to remove all tissue surrounding the bones before homogenizing to prevent contamination of other undesired cell types. During RBC lysis and digestions, it is important to stop the enzymatic reaction with an appropriate amount of FACS Buffer and resuspend thoroughly in fresh buffer, or cells will continue to digest and eventually die.

Separating the bone and bone marrow fractions is essential since the bone spicules require a different mix of enzymes for digestion buffer and need longer time to digest. In bone digestions, the collagenase type 1 is useful for digesting collagenase fibrils which are commonly found in extracellular matrix and collagen fibers[31]. Additionally, some bone marrow cells located close to the endosteum will remain attached to the bone after homogenizing and are only released by enzymatic digestion. When digesting bone marrow, collagenase type IV is used to digest the basement membrane of epithelial and endothelial cells within the bone marrow[32], while dispase mainly cleaves fibronectin[31]. The bone marrow requires less time to digest as the associations between cells and matrix are weaker. Incubating the bone marrow fraction in similar conditions can damage the populations of interest. Using two different digestion buffers significantly increases the number of stomal populations that can be detected, and thus provides a larger data set to analyze.

Most available protocols to analyze murine bone marrow microenvironmental populations use a syringe to flush the bone marrow from only the long bones[13,24]. The current method of crushing bones provides the ability of acquiring data from other bones such as the pelvis, significantly reduces sample preparation time, and mitigates the possibility of injuries with sharp needles. Given that the bone consists of mature osteoblasts and other cell populations that can provide support to normal and malignant hematopoietic cells, this method of including cells from the bone spicules enables a more accurate representation of the bone marrow microenvironment in the sample. While one previous study digested bone marrow and bone spicules separately[11], it did not demonstrate staining of osteolineage and endothelial cells in the same sample. A second study used commercially available proprietary enzyme mixes to digest bone marrow and bone spicules[23], and analyzed the data using the significantly more expensive single cell RNA-sequencing technology. This method of enriching for CD45-/Ter119- cells selects for cells of interest, and significantly reduces the time needed to acquire data on the flow cytometer. Thus, compared to other state of the art methods such as single-cell RNA sequencing, this flow cytometry-based method is more accessible, cost-effective and does not require sophisticated analysis by trained bioinformaticians[23,24,30].

It is important to note that this protocol can be used to characterize the bone marrow microenvironment of not only any of the available murine models of MDS and AML but any genetic mouse model. Similar methods can also be effective in analyzing the changes in the murine bone marrow niche of patient derived xenograft (PDX) models. These methods can be useful for studies aimed at determining the mechanisms by which MDS/AML affect their bone marrow niche. Given the technical challenges associated

with sampling large quantities of bone marrow from human patients, these analyses of murine models are an effective tool to further the understanding of the malignant bone marrow microenvironment and define its role in disease progression.

Disclosures

No conflicts of interest declared.

Acknowledgments

We would like to thank the URMC Flow Cytometry Core. This work was supported by American Society of Hematology Scholar Award, Leukemia Research Foundation award and NIH grants R01DK133131 and R01CA266617 awarded to J.B.

References

1. Morrison, S. J., Scadden, D. T. The bone marrow niche for haematopoietic stem cells. *Nature.* **505** (7483), 327-334 (2014).
2. Boulais, P. E., Frenette, P. S. Making sense of hematopoietic stem cell niches. *Blood.* **125** (17), 2621-2629 (2015).
3. Pinho, S., Frenette, P. S. Haematopoietic stem cell activity and interactions with the niche. *Nat Rev Mol Cell Biol.* **20** (5), 303-320 (2019).
4. Kfoury, Y., Scadden, D. T. Mesenchymal cell contributions to the stem cell niche. *Cell Stem Cell.* **16** (3), 239-253 (2015).
5. Itkin, T. et al. Distinct bone marrow blood vessels differentially regulate haematopoiesis. *Nature.* **532** (7599), 323-328 (2016).
6. Bajaj, J. et al. Cd98-mediated adhesive signaling enables the establishment and propagation of acute myelogenous leukemia. *Cancer Cell.* **30** (5), 792-805 (2016).
7. Konopleva, M. Y., Jordan, C. T. Leukemia stem cells and microenvironment: Biology and therapeutic targeting. *J Clin Oncol.* **29** (5), 591-599 (2011).
8. Kim, Y. W. et al. Defective notch activation in microenvironment leads to myeloproliferative disease. *Blood.* **112** (12), 4628-4638 (2008).
9. Walkley, C. R. et al. A microenvironment-induced myeloproliferative syndrome caused by retinoic acid receptor gamma deficiency. *Cell.* **129** (6), 1097-1110 (2007).
10. Kode, A. et al. Leukaemogenesis induced by an activating β-catenin mutation in osteoblasts. *Nature.* **506** (7487), 240-244 (2014).
11. Hanoun, M. et al. Acute myelogenous leukemia-induced sympathetic neuropathy promotes malignancy in an altered hematopoietic stem cell niche. *Cell Stem Cell.* **15** (3), 365-375 (2014).
12. Raaijmakers, M. H. et al. Bone progenitor dysfunction induces myelodysplasia and secondary leukaemia. *Nature.* **464** (7290), 852-857 (2010).
13. Frisch, B. J. et al. Functional inhibition of osteoblastic cells in an in vivo mouse model of myeloid leukemia. *Blood.* **119** (2), 540-550 (2012).
14. Bajaj, J., Diaz, E., Reya, T. Stem cells in cancer initiation and progression. *J Cell Biol.* **219** (1), e201911053 (2020).
15. Sekeres, M. A., Taylor, J. Diagnosis and treatment of myelodysplastic syndromes: A review. *Jama.* **328** (9), 872-880 (2022).

16. Zeisig, B. B., Kulasekararaj, A. G., Mufti, G. J., So, C. W. Snapshot: Acute myeloid leukemia. *Cancer Cell.* **22** (5), 698-698.e1 (2012).

17. Krivtsov, A. V., Armstrong, S. A. Mll translocations, histone modifications and leukaemia stem-cell development. *Nat Rev Cancer.* **7** (11), 823-833 (2007).

18. Yoshimi, A. et al. Coordinated alterations in rna splicing and epigenetic regulation drive leukaemogenesis. *Nature.* **574** (7777), 273-277 (2019).

19. Lin, Y. W., Slape, C., Zhang, Z., Aplan, P. D. Nup98-hoxd13 transgenic mice develop a highly penetrant, severe myelodysplastic syndrome that progresses to acute leukemia. *Blood.* **106** (1), 287-295 (2005).

20. Kwon, H. Y. et al. Tetraspanin 3 is required for the development and propagation of acute myelogenous leukemia. *Cell Stem Cell.* **17** (2), 152-164 (2015).

21. Bajaj, J. et al. An *in vivo* genome-wide crispr screen identifies the rna-binding protein staufen2 as a key regulator of myeloid leukemia. *Nat Cancer.* **1** (4), 410-422 (2020).

22. Krivtsov, A. V. et al. Transformation from committed progenitor to leukaemia stem cell initiated by mll-af9. *Nature.* **442** (7104), 818-822 (2006).

23. Baryawno, N. et al. A cellular taxonomy of the bone marrow stroma in homeostasis and leukemia. *Cell.* **177** (7), 1915-1932.e16 (2019).

24. Tikhonova, A. N. et al. The bone marrow microenvironment at single-cell resolution. *Nature.* **569** (7755), 222-228 (2019).

25. Balderman, S. R. et al. Targeting of the bone marrow microenvironment improves outcome in a murine model of myelodysplastic syndrome. *Blood.* **127** (5), 616-625 (2016).

26. Au - Amend, S. R., Au - Valkenburg, K. C., Au - Pienta, K. J. Murine hind limb long bone dissection and bone marrow isolation. *JoVE.* **110**, e53936 (2016).

27. JoVE Science Education Database. Basic Methods in Cellular and Molecular Biology. Using a Hemacytometer to Count Cells. *JoVE.* (2023).

28. Passaro, D. et al. Increased vascular permeability in the bone marrow microenvironment contributes to acute myeloid leukemia progression and drug response. *Blood.* **128** (22), 2662 (2016).

29. Xu, C. et al. Stem cell factor is selectively secreted by arterial endothelial cells in bone marrow. *Nat Commun.* **9** (1), 2449 (2018).

30. Baccin, C. et al. Combined single-cell and spatial transcriptomics reveal the molecular, cellular and spatial bone marrow niche organization. *Nat Cell Biol.* **22** (1), 38-48 (2020).

31. Ebrahimi Dastgurdi, M., Ejeian, F., Nematollahi, M., Motaghi, A., Nasr-Esfahani, M. H. Comparison of two digestion strategies on characteristics and differentiation potential of human dental pulp stem cells. *Arch Oral Biol.* **93**, 74-79 (2018).

32. Abreu-Velez, A. M., Howard, M. S. Collagen IV in normal skin and in pathological processes. *N Am J Med Sci.* **4** (1), 1-8 (2012).